Synthesis, Spectroscopy, and Magnetic Properties of Fe^{II} and Co^{II} Quinoline-2-carboxylates − Crystal Structure of *trans*-Bis(quinoline-2-carboxylato)bis(propanol)iron(II)

Danuta Dobrzyńska,*[a] Marek Duczmal,[a] Lucjan B. Jerzykiewicz,[b] Jolanta Warchulska,[c] and Krzysztof Drabent[b]

Keywords: Vibrational spectroscopy / Magnetic properties / Iron / Cobalt / Quinoline-2-carboxylates

The new coordination compounds, $[Fe(quin\text{-}2\text{-}c)_2(EtOH)_2]$ (**1**), $[Co(quin\text{-}2\text{-}c)_2(EtOH)_2]$ (**2**), and $[Fe(quin\text{-}2\text{-}c)_2(PrOH)_2]$ (**3**) (where quin-2-c = quinoline-2-carboxylate) have been synthesized and investigated by ligand field, IR, Raman, and Mössbauer spectroscopy and by magnetic measurements. The X-ray analysis of the structure of **3** has been performed and refined to an *R* factor of 0.0377. The compound crystallizes in the monoclinic space group $P2_1/n$ with a = 6.104(1), b = 10.515(2), c = 19.339(4) Å, β = 92.57(3)°. The *trans* N_2O_4 environment around the Fe^{II} ion has a distorted octahedral geometry and the quin-2-c ion coordinates to iron in the equatorial plane in a chelating mode. The axial positions are occupied by propan-1-ol molecules. The spectral studies indicate the same molecular structure for all three compounds. The magnetic susceptibility and the magnetization of **2** were calculated for Co^{2+} ions in an octahedral crystal field with a rhombic zero field distortion ($|D|$ = 34 cm^{-1}, $E \approx 0$, g_{iso} = 2.35 and $N = 6.9 \cdot 10^{-4}$ emu·mol^{-1}).

Introduction

Carboxylate ligands are ubiquitous in biological materials and common in systems of catalytic utility. The carboxylate group offers a variety of coordination modes and many types of complexes are known.[1] Many of them, with interesting magnetic properties, have been obtained and characterized.[2]

Quinoline-2-carboxylic acid is a strong chelating agent and has been used as a reagent for the gravimetric determination of copper, cadmium, zinc and palladium.[3,4] In complexes with Rh^{I},[5−8] Rh^{III},[9] Mn^{II},[10,11] Cu^{II},[12] Ga^{III},[13] and Zn^{II}.[14] X-ray studies have revealed an N,O coordination mode of the quinoline-2-carboxylate ion. In chlorotriphenyl(quinolinium-2-carboxylato-*O*)tin(IV) monohydrate a quinoline-2-carboxylic acid binds to tin in its zwitterionic form.[15] The neutral acid molecule is demonstrated in the structure of bis(quinoline-2-carboxylic acid)tetrabromogold(III) monohydrate.[16] In the $Nd_2L_6{\cdot}3H_2O$ dimer, the coordinated quinoline-2-carboxylate ions display three modes of bonding: a bidentate carboxylate bridge, an O,O and an N,O chelating mode.[17]

It is interesting that the carboxylate group in the position *ortho* to the quinoline nitrogen, present in quin-2-c, is essential for binding Ca^{2+} and Fe^{2+} in PQQ (pyrroloquinilnequinone) which is involved as co-factor in enzymes of the quinoprotein group.[18]

In this paper, we describe the synthesis, spectroscopic and magnetic studies of low molecular weight, neutral complexes of iron(II) and cobalt(II) with the quionoline-2-carboxylate ion. The crystal structure of the ferrous compound is also presented.

Results and Discussion

Description of the Structure

The molecular geometry of $[Fe(quin\text{-}2\text{-}c)_2(PrOH)_2]$ (**3**) is shown in Figure 1, and Figure 2 (a) shows the crystal packing. Table 1 lists selected bond lengths and angles.

In the molecule of **3**, the iron(II) is six-coordinate with an O_4N_2 donor set. The coordination sphere can be described as distorted ocahedral. Two quin-2-c ligands coordinate to iron in the O,N chelating mode in the equatorial plane. The axial positions are occupied by the propanol molecules. The complex has an inversion center at the Fe^{II} ion. The Fe−O(1) bond length of 2.033(2) Å is short in comparison with the data found for iron(II) dipicolinates,[19−21] picolin-

[a] Institute of Inorganic Chemistry and Metallurgy of Rare Elements, Wrocław University of Technology,
Wybrzeże Wyspiańskiego 27, 50−370 Wrocław, Poland
Fax: (internat.) +48-(0)71-3284330
E-mail: dobrzynska@ichn.ch.pwr.wroc.pl
[b] Faculty of Chemistry, University of Wrocław,
Joliot-Curie 14, 50−383 Wrocław, Poland
[c] International Laboratory of High Magnetic Fields and Low Temperatures,
Gajowicka 95, 53−529 Wrocław, Poland

  DOI: 10.1002/ejic.200300327

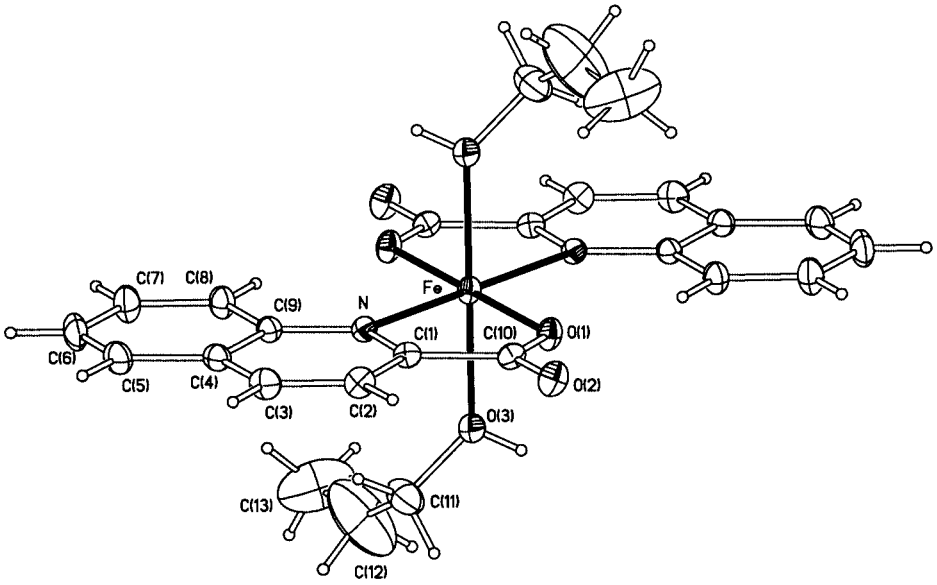

Figure 1. The molecular structure of $[Fe(quin\text{-}2\text{-}c)_2(PrOH)_2]$ with atom numbering scheme; the displacement ellipsoids are drawn at the 50% probability level

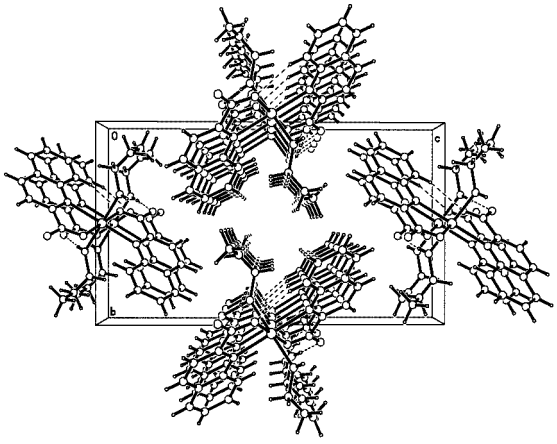

(a)

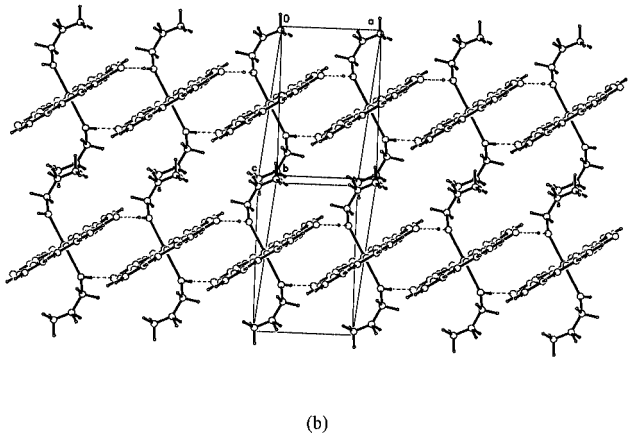

(b)

Figure 2. (a) The crystal packing of **3** viewed down the *a* axis; (b) the 1D-chains of $[Fe(quin\text{-}2\text{-}c)_2(PrOH)_2]$ molecules connected through the $O(2)^{ii}\cdots H(3O)-O(3)$ hydrogen bonds (indicated by the dashed lines)

ates,[22] and *bis*(isonicotinato)iron(II),[23] which cover the range 2.05(1)−2.37(1) Å. The Fe−N distance of 2.246(2) Å is similar to those found in ferrous dipicolinates[21] and picolinates[22] and is characteristic of high-spin Fe^{II} complexes.[24] The Fe−O(3) bond length is 2.170(3) Å. This distance is slightly shorter than the Fe^{II}−O(H)Me bond in iron(II) alkoxide cubes [2.24(2) and 2.208(2) Å][25] and in $[Fe(Pic)_2(MeOH)_2]$ [2.208(1) Å].[22]

The quinoline rings are coplanar with the equatorial chelate rings. This plane of the complex is stabilized by the weak C−H···O type intramolecular interaction [the $C(8)\cdots O(1)^{i}$ distance is 3.179(4) Å, the $C(8)-H(8)\cdots O(1)^{i}$ angle is 154(1)°, i = $-x$, $-y$, $-z$ + 1, Table 2]. Each carbonyl oxygen of the carboxylate group acts as an acceptor, resulting in a strong hydrogen bond with the hydroxyl group of the coordinated propanol molecule of an adjacent complex [the $O(2)^{ii}\cdots O(3)$ distance is 2.659(4) Å, the $O(2)^{ii}\cdots H(3O)-O(3)$ angle is 177(5)°, ii = $-x$ + 1, $-y$, $-z$ + 1]. This intermolecular interaction links the molecules into an infinite 1D-chain along the *a* axis (Figure 2, b). The Fe···Fe distance in the chain is 6.104(1) Å. In the crystal, interactions occur between the aromatic rings of the quinoline units (3.5 Å separation in stack).

Vibrational Spectra

The bands observed in the IR spectra of $[Fe(quin\text{-}2\text{-}c)_2(EtOH)_2]$ (**1**), $[Co(quin\text{-}2\text{-}c)_2(EtOH)_2]$ (**2**), and $[Fe(quin\text{-}2\text{-}c)_2(PrOH)_2]$ (**3**) and in the Raman spectrum of **2** as well as tentative assignments of these bands are given in Table 3. The IR spectra of $[Fe(quin\text{-}2\text{-}c)_2(EtOH)_2]$ and $[Co(quin\text{-}2\text{-}c)_2(EtOH)_2]$ are very similar in terms of the frequency, intensity and shape of the bands over the whole frequency region. The spectra are dominated by strong bands resulting from quinoline-2-carboxylate oscillations, but sev-

Table 1. Bond lengths and angles for $[Fe(quin\text{-}2\text{-}c)_2(PrOH)_2]$ (**3**) (i: symmetry transformations used to generate equivalent atoms: $-x$, $-y$, $-z + 1$)

Fe−O(1)	2.033(2)
Fe−O(3)	2.170(3)
Fe−N	2.246(2)
O(1)−C(10)	1.262(3)
O(2)−C(10)	1.233(3)
O(3)−C(11)	1.385(5)
N−C(1)	1.326(4)
N−C(9)	1.370(4)
C(1)−C(2)	1.402(4)
C(1)−C(10)	1.509(4)
C(2)−C(3)	1.361(5)
C(3)−C(4)	1.397(5)
C(4)−C(5)	1.419(5)
C(4)−C(9)	1.420(4)
C(5)−C(6)	1.344(5)
C(6)−C(7)	1.397(5)
C(7)−C(8)	1.362(5)
C(8)−C(9)	1.405(4)
C(11)−C(12)	1.334(9)
C(12)−C(13)	1.200(12)
O(1)−Fe−O(3)	91.14(10)
O(1)−Fe−O(3)^{i}	88.86(10)
O(1)−Fe−N	77.12(9)
O(1)^{i}−Fe−N	102.88(9)
O(3)−Fe−N	94.04(9)
O(3)^{i}−Fe−N	85.96(9)
O(1)−Fe−N^{i}	102.88(9)
C(10)−O(1)−Fe	119.32(19)
C(11)−O(3)−Fe	129.4(3)
C(1)−N−C(9)	118.3(2)
C(1)−N−Fe	109.92(18)
C(9)−N−Fe	131.79(19)
N−C(1)−C(2)	123.1(3)
N−C(1)−C(10)	116.6(2)
C(2)−C(1)−C(10)	120.3(3)
C(3)−C(2)−C(1)	119.5(3)
C(2)−C(3)−C(4)	119.4(3)
C(3)−C(4)−C(5)	122.9(3)
C(3)−C(4)−C(9)	118.4(3)
C(5)−C(4)−C(9)	118.7(3)
C(6)−C(5)−C(4)	120.0(3)
C(5)−C(6)−C(7)	121.3(3)
C(8)−C(7)−C(6)	120.8(3)
C(7)−C(8)−C(9)	119.8(3)
N−C(9)−C(8)	119.3(3)
N−C(9)−C(4)	121.3(3)
C(8)−C(9)−C(4)	119.4(3)
O(2)−C(10)−O(1)	125.3(3)
O(2)−C(10)−C(1)	117.9(3)
O(1)−C(10)−C(1)	116.9(2)
C(12)−C(11)−O(3)	118.3(7)
C(13)−C(12)−C(11)	143.3(14)

Table 2. Hydrogen bonds for $[Fe(quin\text{-}2\text{-}c)_2(PrOH)_2]$ (**3**) (symmetry transformations used to generate equivalent atoms: i: $-x$, $-y$, $-z + 1$. ii: $-x + 1$, $-y$, $-z + 1$)

D−H···A	D−H	H···A	D···A	∠ D−H···A
O(3)−H(3O)···O(2)^{ii}	0.79(4)	1.87(4)	2.659(4)	177(5)
C(8)−H(8)···O(1)^{i}	0.930(4)	2.311(2)	3.179(4)	154(1)

eral bands characteristic of vibrations due to ethanol are also observed. Differences between these two spectra are observed in the low frequency region and are related to the bands generated by the vibrations of metal−ligand bonds.

The IR spectrum of $[Fe(quin\text{-}2\text{-}c)_2(PrOH)_2]$ is in very good agreement with the spectrum of $[Fe(quin\text{-}2\text{-}c)_2(EtOH)_2]$ in terms of the bands resulting from vibrations of the quin-2-c ion and vibrations of the coordination bonds. In particular, the bands found in the regions 1630−1150 cm^{-1} and 900−750 cm^{-1} have the same positions, intensities and shapes. The bands related to the propan-1-ol vibrations are easily found in the spectrum of **3** (Table 3).

The features which make the spectra of **1** and **2** distinct from that of **3**, apart from the previously mentioned alcohol and coordination modes, are two weak and broad bands observed near 3400 cm^{-1} and 700 cm^{-1} seen only for the ethanolic adducts. We have attributed these bands to the vibrations of trace amounts of water, $\nu(H_2O)$ and $\rho_w(H_2O)$, respectively. The positions and shapes of these bands are characteristic of coordinated water molecules.[26,27] The lower quality crystals of **1** and **2** compared with those of **3** may result from disorder in the crystals caused by the trace amounts of water. The absence of the above mentioned bands near 3400 cm^{-1} and 700 cm^{-1} in the IR spectrum of the propanol adduct **3**, the structure of which is presented here, supports our assignment.

The bands generated by the ν(OH) vibrations of alcohols are expected over a wide frequency range (3400−2500 cm^{-1}) with the frequencies considerably dependent on hydrogen bonding.[28] In the crystal of **3** the hydroxyl group of the coordinated propan-1-ol molecule forms a strong hydrogen bond with the carbonyl oxygen atom from the carboxylate group of neighbouring molecule. On this basis we have assigned the vibrations of the hydrogen bond in **3** to the medium bands observed at 2686 and 2574 cm^{-1} in its IR spectrum. The hydrogen bonding modes may also contribute to the group of strong and closely spaced bands at higher frequencies (3200−2800 cm^{-1}), but as a result of overlapping with the $\nu(C-H)_{aliph}$ and $\nu(C-H)_{arom}$ absorptions, their frequencies cannot be resolved. In the spectra of **1** and **2,** in the region 2750−2500 cm^{-1}, two doublets can be observed repeating the intensity pattern seen in the spectrum of **3** (see Table 2). These can be attributed to hydrogen bonding involving the OH group from the ethanol molecule.

The characteristic bands due to the vibrations of alcohols [with exception of the ν(OH) mode] are observed in the regions of 3100−2800 cm^{-1} [$\nu(CH_3)$ and $\nu(CH_2)$] 1100−900 cm^{-1} [ν(CO) and CH_3, CH_2 deformations] and 500−400 cm^{-1} (deformations of the C−C−O fragment) in the IR spectra of all complexes.

Inspection of the IR region 1630−1300 cm^{-1} indicates that the carboxylate group coordination mode is the same for all complexes. The values of $\Delta\nu(CO_2) = \nu_{as}(CO_2) - \nu_s(CO_2)$ are equal to 232, 225, and 234 cm^{-1} for **1**, **2**, and **3**, respectively, and indicate that the carboxylate group binds in a monodentate fashion.[29]

Table 3. The frequencies observed in the IR spectra of $[Fe(quin\text{-}2\text{-}c)_2(EtOH)_2]$ (**1**), $[Co(quin\text{-}2\text{-}c)_2(EtOH)_2]$ (**2**), and $[Fe(quin\text{-}2\text{-}c)_2(PrOH)_2]$ (**3**) and in the Raman spectrum of **2** [cm^{-1}] and their assignment; assignment of quinoline ring vibrations was made according to Bellamy;[28] abbreviations: vs − very strong, s − strong, m − medium, w − weak, vw − very weak, b − broad, sh − shoulder, et − ethanol, prop − propanol

1 IR	2 IR	3 IR	2 R	Assignment
3386 mb	3433 mb			$\nu(H_2O)$
3064 vs	3068 m	3060 vs	3069 m	$\nu(C-H)_{quin}$
3045 s	3050 s		3054 m	$\nu(CH_3)$, $\nu(CH_2)$
3000 s,sh	3010 s,sh		3012 w	$\nu(CH_3)$, $\nu(CH_2)$
2963 vs	2964 m	2956 vs	2954 m	$\nu(CH_3)$, $\nu(CH_2)$
2916s	2920 s	2932 vs	2921 m	$\nu(CH_3)$, $\nu(CH_2)$
2905s	2907 s			$\nu(CH_3)$, $\nu(CH_2)$
2884 s	2883 s	2865 vs	2878 m	$\nu(CH_3)$, $\nu(CH_2)$
2836 vs	2813 s	2833 vs		$\nu(CH_3)$, $\nu(CH_2)$
2734 m	2735 m	2686 m		hydrogen bond vibrations
2710 m	2712 m			hydrogen bond vibrations
2584 m	2588 w	2575 m		hydrogen bond vibrations
2570 m	2561 w			hydrogen bond vibrations
1628 vs	1627 vs	1628 vs	1620 vw	$\nu(COO)_{as}$
1596 vs	1600 s	1595 s	1595 m	$\nu(C-C)$, $\nu(C-N)$ and $\delta(C-H)$ vibrations of the quinoline fragment
1564 s	1564 s	1563 s	1565 vw	$\nu(C-C)$, $\nu(C-N)$ and $\delta(C-H)$ vibrations of the quinoline fragment
1548 s	1552 m	1551 m	1547 vw	$\nu(C-C)$, $\nu(C-N)$ and $\delta(C-H)$ vibrations of the quinoline fragment
1509 m	1509 m	1509 m	1507 vw	$\nu(C-C)$, $\nu(C-N)$ and $\delta(C-H)$ vibrations of the quinoline fragment
1464 s	1466 s	1464 m	1465 m	$\nu(C-C)$, $\nu(C-N)$ and $\delta(C-H)$ vibrations of the quinoline fragment
1433 s	1432 m	1433 m	1434 w	$\nu(C-C)$, $\nu(C-N)$ and $\delta(C-H)$ vibrations of the quinoline fragment
1395 vs	1396 vs	1394 vs		$\nu(COO)_s$
1378 s	1378 s	1378 ssh	1370 vs	Ring breathing mode
1349 m	1348 m	1349 m		$\nu(C-N)$, $\nu(C-C)$ and $\delta(C-H)$ vibrations of the quinoline fragment
1301 vw	1300 vw	1300 vw		$\nu(C-N)$, $\nu(C-C)$ and $\delta(C-H)$ vibrations of the quinoline fragment
1273 w	1274 w	1274 w	1300 w	$\nu(C-N)$, $\nu(C-C)$ and $\delta(C-H)$ vibrations of the quinoline fragment
1263 vw	1265 w	1264 w	1279 vw	$\nu(C-N)$, $\nu(C-C)$ and $\delta(C-H)$ vibrations of the quinoline fragment
1218 w	1220 vw	1240 vw		$\nu(C-N)$, $\nu(C-C)$ and $\delta(C-H)$ vibrations of the quinoline fragment
1209 w	1211 vw	1215 vw		$\nu(C-N)$, $\nu(C-C)$ and $\delta(C-H)$ vibrations of the quinoline fragment
		1204 w		$\nu(C-N)$, $\nu(C-C)$ and $\delta(C-H)$ vibrations of the quinoline fragment
1181 w	1180 w	1182 w		$\delta(C-H)_{quin}$
1155 m	1154 w	1153 m		$\delta(C-H)_{quin}$
1146 w	1144 vw	1142 vw	1142 vw	
1138 vw	1135 vw	1130 vw		
1120 vw	1118 vw	1115 vw		
1098 m	1097 w	1098 vw		deformation $(CH_3)_{et,\ prop}$
		1074 m		
1056 s	1057 m	1058 m		$\nu(CO)_{et,\ prop}$
1027 w	1027 w	1020 w	1025 w	in-plane deformation modes of the quinoline ring
995 w	997 vw	995 vw		in-plane deformation modes of the quinoline ring
977 w	977 vw			in-plane deformation modes of the quinoline ring
964 w	965 w			in-plane deformation modes of the quinoline ring
902 m	903 m	902 m		in-plane deformation modes of the quinoline ring
885 m	888 w	887 w		$\nu(C-C)_{et,\ prop}$
865 m	867 m	865 m		
809 s	810 m	810 m		$\gamma(C-H)_{quin}$
781 vs	781 s	781 s	779 m	$\gamma(C-H)_{quin}$
752 vw	750 vw	751 vw		
699 vw,b	712 vw,b			$\rho_w(H_2O)$
634 m	636 m	634 w		
605 s	605w	605 m		$\delta(C=O)$
560 vw	563 vw	556 vw		out-of-plane deformations of the quinoline ring
521 w	522 w	522 w	524 w	out-of-plane deformations of the quinoline ring
502 m	503 m	503 m		out-of-plane deformations of the quinoline ring
485 vw	485 vw	485 vw		out-of-plane deformations of the quinoline ring
		472 w		$\delta(CCO)_{prop}$
		464 w		$\delta(CCC)_{prop}$
435 vw	435 w			$\delta(CCO)_{et}$
406 m	406 s	407 m	406 w	deformation mode of the quinoline rings
399 m	406 s	398 m		$\nu(M-O_{carbox})$
385 s	390 s	387 s		$\nu(M-O_{alc})$
317 m	321 s	319 m		def. mode of the quinoline rings
		264 w		
239 w	247 m	238 w		$\nu(M-N)$
204 s	205 s	205 s		deformation modes
152 m	165 m	157 w	158 m	deformation modes

The energies of the stretching vibrations of the iron(II)-aromatic nitrogen are indicative of the spin state of the ferrous ion. The ν(Fe−N) vibrations can be observed in the range 250−220 cm^{-1} for high-spin and 530−370 cm^{-1} for low spin complexes.[30,31] In the IR spectra of **1** and **3** the ν(Fe−N) mode generates the bands located at 239 cm^{-1} and 238 cm^{-1}, respectively. The positions of the bands due to the metal-oxygen bond vibrations according to Nakamoto[27] are listed in the Table 3.

Comparison of the IR and Raman spectra of **1** and **2** with that of **3** leads to the conclusion that the molecular structures of the three complexes are very similar. Two quin-2-c ions occupy the equatorial positions and coordinate to the metal in a chelating mode via the carboxylate group and the aromatic nitrogen atom. The axial positions are occupied by two propan-1-ol molecules in **3** and by molecules of ethanol and trace amounts of water in **1** and **2**.

Electronic Spectra and Magnetic Properties

The maximum observed in the ligand field spectrum of $[Fe(quin\text{-}2\text{-}c)_2(EtOH)_2]$ at $9.5\cdot10^3$ cm^{-1} is characteristic of high spin iron(II) octahedral complexes.[32] This absorption can be attributed to the spin allowed $^5E_g \leftarrow {}^5T_{2g}(D)$ transition. A strong band, centered at $18.0\cdot10^3$ cm^{-1}, arises from an iron→ligand CT absorption. The ligand field absorption bands in the cobalt complex are found at about 8.41, 18.6, 20.9, and $22.3\cdot10^3$ cm^{-1}. These bands are commonly observed for six coordinate high-spin Co^{II} complexes.[32]

The structure of the framework of magnetic ions in $[Fe(quin\text{-}2\text{-}c)_2(PrOH)_2]$ consists of linear chains of Fe^{2+} ions along the *a* axis [Figure 2 (b)]. The M−M distance of 6.104(1) Å is rather long, precluding any direct magnetic exchange interactions. However the strong hydrogen bonds between the molecules in the chain [O(3)−H(3O)···O(2)^{ii}] make indirect interactions possible. The distance between the neighbouring chains is larger than 10 Å and the spatial arrangement of the ligands seems to rule out an effective pathway for inter-chain magnetic exchange.

The magnetic susceptibilities of $[Fe(quin-2\text{-}c)_2(EtOH)_2]$ and $[Fe(quin\text{-}2\text{-}c)_2(PrOH)_2]$ obey the Curie−Weiss law above ca. 50 K with the positive Weiss constants (+2.6 K and +7.0 K for **1** and **3**, respectively) and large magnetic moments (5.22 μ_B and 5.22 μ_B, calculated from the Curie−Weiss formula) characteristic of high-spin iron(II) complexes [Figure 3 shows the results for $[Fe(quin\text{-}2\text{-}c)_2(PrOH)_2]$. The results for $[Fe(quin\text{-}2\text{-}c)_2(EtOH)_2]$ are quite similar].

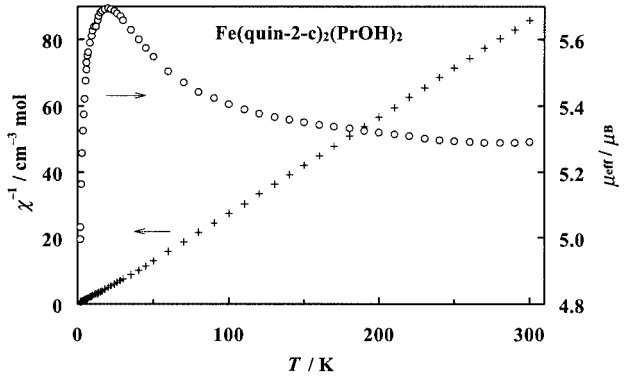

Figure 3. Temperature dependence of reciprocal susceptibility (+) and the effective magnetic moment (o) for the polycrystalline sample of $[Fe(quin\text{-}2\text{-}c)_2(PrOH)_2]$ (H = 5000 Oe)

The effective magnetic moments of the iron compounds increase with desreasing temperature, reach broad maxima at 23 K (**1**) and 20 K (**3**), then decreases quickly below T_{max}. Such behaviour is characteristic of complexes with ferro- or ferrimagnetic exchange interactions.[33] The field dependence of the magnetizations is also interesting (Figure 4). Both compounds show hysteresis at 1.9 K with the zero magnetic remanence. Similar curves have been observed for metamagnetic compounds, for example $Fe(N_2H_5)_2(SO_4)_2$.[34]

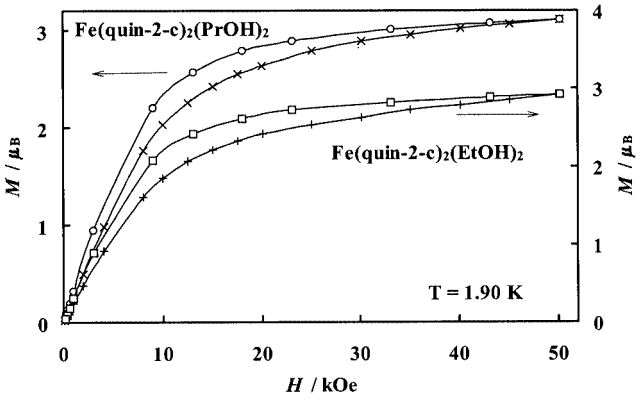

Figure 4. Field dependence of magnetization at 1.90 K for $[Fe(quin\text{-}2\text{-}c)_2(PrOH)_2]$ and $[Fe(quin\text{-}2\text{-}c)_2(EtOH)_2]$; crosses − increasing field, circles and squares − decreasing field

The magnetic properties of the iron complexes do not have a satisfactory explanation. A long-range order, which may be considered as an explanation of the behaviour of isothermal magnetization (Figure 4), is not possible in a pure one-dimensional network. However, it is not easy to see any obvious pathway for the interchain magnetic exchange. A more detailed analysis of the magnetic data is beyond the scope of this article and will be presented elsewhere.

The magnetic properties of the cobalt compound are different from those of the iron complexes. The properties of $[Co(quin\text{-}2\text{-}c)_2(EtOH)_2]$ are rather typical. The magnetic susceptibility obeys the Curie−Weiss law down to about 30 K (Figure 5). The parameters of the C−W equation depend on the Van Vleck temperature-independent paramagnetism ($N\alpha$), which is usually strong for high-spin Co^{2+} compounds.[35,36] If we assume $N\alpha = 6.9\cdot10^{-4}$ emu mol^{-1}, obtained from the fitting of the calculated and the experimental μ_{eff} (see below), the values μ = 4.57 μ_B and θ = −3.0 K are obtained (μ = 4.84 μ_B and θ = −15.6 K are found for the uncorrected susceptibility). The effective magnetic moment decreases monotonically between room temperature and 1.9 K, changing from 4.75 to 3.62 μ_B. The field dependence of magnetization shows no hysteresis and the

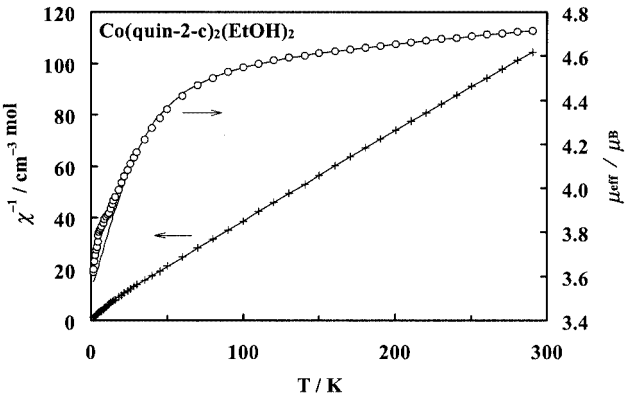

Figure 5. Temperature dependence of reciprocal susceptibility (+) and the effective magnetic moment (o) for the polycrystalline sample of $[Co(quin\text{-}2\text{-}c)_2(EtOH)_2]$ (H = 5000 Oe); the lines were calculated for S = 3/2 with the ZFS parameter $|D|$ = 34 cm^{-1}, g = 2.35 and $N\alpha = 6.9\cdot10^{-4}$ $cm^3\cdot mol^{-1}$

magnetization is almost saturated at 1.9 K in a field of 50 kOe, reaching a value of 2.2 μ_B (Figure 6).

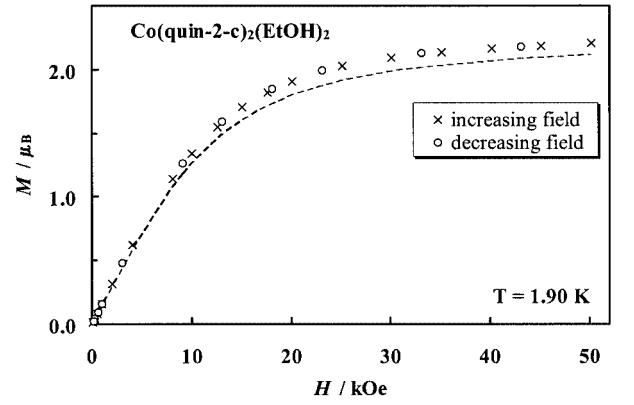

Figure 6. Field dependence of magnetization at 1.90 K for $[Co(quin\text{-}2\text{-}c)_2(EtOH)_2]$; the dashed line represents the ZFS magnetization with $|D|$ = 34 cm^{-1}, $E \approx 0$, $g_z = g_x = g_y$ = 2.35 and the Van Vleck contribution $N\alpha = 6.9\cdot10^{-4}$ $cm^3\cdot mol^{-1}$

In contrast to the iron compounds, magnetic exchange interactions are not well pronounced in the experimental results for $[Co(quin\text{-}2\text{-}c)_2(EtOH)_2]$. We therefore tried to apply the model of isolated Co^{2+} ions in the octahedral crystal field deformed by the rhombic zero field distortion. Taking into account only the second-order crystal field parameters, the spin Hamiltonian can be written as [Equation(1)], where S = 3/2.

$$H = g_z\cdot\beta\cdot H\cdot S_z + D\cdot[S_z^2 - 1/3\cdot S\cdot(S+1)] + E\cdot(S_x^2 - S_y^2) \quad (1)$$

The appropriate matrix elements and the relations between the parameters of the Hamiltonians with the different field directions were given by Abragam and Bleaney.[37] The least-squares refinement of the temperature dependence of μ_{eff} yielded $|D|$ = 34 cm^{-1}, $E \approx 0$, $g_z = g_x = g_y$ = 2.35 and the Van Vleck contribution $N\alpha = 6.9\cdot10^{-4}$ $emu\cdot mol^{-1}$. The calculated curve fits the experimental points well at higher temperatures. Below 30 K the calculated points deviate slightly from the experimental ones (Figure 5).

Moreover, the field dependence of magnetization is fairly well described by this set of parameters (Figure 6). There are at least two possible reasons of the low-temperature discrepancies: neglecting the fourth-order crystal-field parameters[38,39] and the appearance of weak magnetic exchange effects in the lowest temperature range. The large value of the axial ZFS parameter D is not unusual for Co^{2+} complexes. For example, in $Cd_2P_2S_6:Co^{2+}$ with trigonally distorted CoS_6 octahedra D = 63 cm^{-1} and it reaches a value of 84 cm^{-1} for the more covalent $Cd_2P_2Se_6:Co^{2+}$.[40,41]

The Mössbauer spectrum of $[Fe(quin\text{-}2\text{-}c)_2(EtOH)_2]$ recorded at 293 K consists of an unsymmetrical quadrupole split doublet, Figure 7.

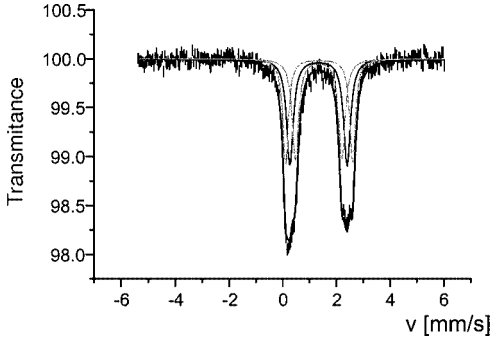

Figure 7. Room temperature Mössbauer spectrum of $[Fe(quin\text{-}2\text{-}c)_2(EtOH)_2]$

The observed asymmetry of the Mössbauer doublet cannot be attributed to the metal−metal interaction because the magnetic susceptibility data indicate that the ferrous ions are isolated. However the crystal structure of **1** is not known, although we can expect that the Fe−Fe distance in **1** is similar to that found in **3** [6.104(1) Å]. According to the least squares fitting with Lorenz curves, the Mössbauer spectrum of $[Fe(quin\text{-}2\text{-}c)_2(EtOH)_2]$ was resolved into three quadrupole doublets with *IS*, *QS*, and Γ parameters (Table 4) being very close to each other. This indicates that in the studied sample, three complexes of Fe^{II} are present having the same donor set and the same geometry. The parameters of the three components of the quadrupole split doublet are characteristic of high-spin iron(II) in an N_2O_4 octahedral environment.[18,19−21,23] The results of the Mössbauer study are consistent with the IR data and demonstrate that three compounds appear in the crystal of **1**, namely $[Fe(quin\text{-}2\text{-})_2(EtOH)_2]$, $[Fe(quin\text{-}2\text{-}c)_2(H_2O)_2]$, and $[Fe(quin\text{-}2\text{-}c)_2(EtOH)(H_2O)]$.

Table 4. Mössbauer data for $[Fe(quin\text{-}2\text{-}c)_2(EtOH)_2]$

	IS [mm/s]	*QS* [mm/s]	Γ/2 [mm/s]
I	1.378(3)	2.13(1)	0.15(3)
II	1.381(3)	1.73(1)	0.12(1)
III	1.38(1)	2.52(1)	0.14(1)

Experimental Section

Safety Note: Perchlorates are potentially explosive. Although we have experienced no accidents so far, all compounds containing perchlorate should be handled with care and in small quantities.

***trans*-Bis(quinoline-2-carboxylato)bis(ethanol)iron(II) (1):** A solution of $Fe(ClO_4)_2 \cdot 6H_2O$ (0.100 g; 0.275 mmol) in ethanol (50 cm^3) was added to a solution of quinoline-2-carboxylic acid (0.095 g, 0.55 mmol) in ethanol (100 cm^3) at room temperature under aerobic conditions. The resultant deep red solution was allowed to stand for two days. During this period crystals of [Fe(quin-2-c)$_2$(EtOH)$_2$] appeared. The dark violet crystals were filtered, washed with ethanol and left to dry in air. Attempts to obtain X-ray quality crystals of this compound were unsuccessful. $C_{24}H_{24}FeN_2O_6$: calcd. C 58.55, H 4.89, N 5.69, Fe 11.34; found C 58.74, H 5.04, N 5.80, Fe 11.03.

***trans*-Bis(quinoline-2-carboxylato)bis(ethanol)cobalt(II) (2):** [Co(quin-2-c)$_2$(EtOH)$_2$] was obtained by a modification of the method reported for Co(quin-2-c)$_2 \cdot 1/2H_2O$.[13] A solution of $CoCl_2 \cdot 6H_2O$ (0.065 g, 0.275 mmol) in ethanol (50 cm^3) was added to a solution of quinoline-2-carboxylic acid (0.095 g, 0.55 mmol) in ethanol (100 cm^3) at room temperature. After two days pink-yellow crystals appeared. The crystals were filtered, washed with water and left to dry in air. Attempts to obtain X-ray quality crystals of this compound were unsuccessful. $C_{24}H_{24}CoN_2O_6$: calcd. C 58.19, H 4.88, N 5.65, Co 11.90; found C 58.01, H 5.20, N 5.65, Co 11.44.

***trans*-Bis(quinoline-2-carboxylato)bis(propanol)iron(II) (3):** A solution of $Fe(ClO_4)_2 \cdot 6H_2O$ (0.100 g; 0.275 mmol) in propanol (50 cm^3) was added to a solution of quinoline-2-carboxylic acid (0.095 g, 0.55 mmol) in propanol (100 cm^3) at room temperature under aerobic conditions. The resultant deep red solution was allowed to stand for two days. During this period crystals of [Fe(quin-2-c)$_2$(PrOH)$_2$] appeared. The dark violet, X-ray quality crystals were filtered, washed with propanol and left to dry in air. $C_{26}H_{28}FeN_2O_6$: calcd. C 60.01, H 5.42, N 5.38, Fe 10.73; found C 60.49, H 5.22, N 5.68, Fe 11.01.

Physical Measurements

Elemental Analyses were performed in the Analytical Laboratory, Department of Chemistry, Wrocław University of Technology.

Magnetic susceptibility down to 1.9 K and magnetization up to 50 kOe were measured with a Quantum Design SQUID magnetometer. Diamagnetic corrections were calculated using Pascal's constants[42] and were found to be $-283 \cdot 10^{-6}$ emu·mol^{-1}, $-282 \cdot 10^{-6}$ emu·mol^{-1}, and $-306 \cdot 10^{-6}$ emu·mol^{-1} for **1**, **2**, and **3**, respectively.

IR spectra were recorded in KBr pellets or nujol mulls using Perkin−Elmer FTIR-2000 and Perkin−Elmer FTIR-1600 spectrophotometers in the frequency range 50−4000 cm^{-1}. The Raman spectra of solid samples were recorded in the range 0−3600 cm^{-1} with a Bruker FIS-88 TRA-10G-Raman instrument. The excitation was provided by a diode pumped neodymium laser at 1064 nm (150 mV Nd:YAG).

Solid state UV/Vis spectra of the powdered samples were measured in the diffuse reflectance mode on a Carry 500 Scan (Varian) UV/Vis/NIR spectrophotometer.

The Mössbauer spectra of a powdered sample of [Fe(quin-2-c)$_2$(EtOH)$_2$] were recorded on a Mössbauer 2330 spectrophotometer (Polon, Poland). The isomer shift values were referenced to a sodium nitroprusside (SNP) standard. ^{57}Co in the Rh matrix of 10 mCi activity was used as the source. The spectra were processed numerically by distribution into Lorenz curves.

X-ray crystallographic Study: Crystal data collection and refinement are summarized in Table 5. Preliminary examination and intensity data collections were carried out on a KUMA KM-4 κ-axis diffractometer with graphite-monochromated Mo-K_α radiation. All data were corrected for Lorentz and polarization effects. Data reduction and analysis were carried out with the Kuma Diffraction programs.[43] The structures were solved by direct methods[44] and refined by the full-matrix least-squares method on all F^2 data using the SHELXL-97 software.[45] After refinement with isotropic displacement parameters for all atoms, an absorption correction was also applied. Carbon-bonded hydrogen atoms were included in calculated positions and refined in the riding mode using the SHELXL-97 default parameters. Other hydrogen atoms were located in a difference map and refined freely. All non-hydrogen atoms were refined with anisotropic displacement parameters.

CCDC-210965 contains the supplementary crystallographic data for this paper. These data can be obtained free of charge at www.ccdc.cam.ac.uk/conts/retrieving.html [or from the Cambridge Crystallographic Data Centre, 12 Union Road, Cambridge

Table 5. Crystal data and structure refinement for [Fe(quin-2-c)$_2$(PrOH)$_2$] (**3**)

Compound	$C_{26}H_{28}FeN_2O_6$
Empirical formula	$2\times(C_{13}H_{14}Fe_{0.50}NO_3)$
Molecular mass	520.35
λ [Å]	0.71073
T [K]	100(1)
Space group	$P2_1/n$
Crystal system	monoclinic
Unit cell dimensions:	
a [Å]	6.104(1)
b [Å]	10.515(2)
c [Å]	19.339(4)
β [°]	92.57(3)
V [Å^3]	1240.0(4)
Z	2
$D_{calcd.}$ [Mg/m^3]	1.394
F(000)	544
Habit	block
Crystal size [mm]	0.5×0.4×0.4
μ [mm^{-1}]	0.652
Absorption correction	Empirical (SHELXA)
Max. and min. transmission	0.9120 and 0.6916
Diffractometer	Kuma KM4 automatic diffractometer
Diffraction geometry	profile data from ω−2θ scans
θ range [°]	2 to 25
Number of reflections measured	2099
Number of unique reflections	1942
$R_{(int.)}$	0.0170
Number of observed reflections	1534 [$I > 2\sigma(I)$]
Refinement method	least-squares on F^2
Final R indices [$I > 2\sigma(I)$]	$R_1 = 0.0377$,[a] $wR_2 = 0.1022$[b]
Final R indices (all data)	$R_1 = 0.0552$,[a] $wR_2 = 0.1097$[b]
Goodness-of-fit (S)	1.046
Largest diff. peak and hole [e·Å^{-3}]	0.519 and −0.354

[a] $R_1 = \Sigma||F_o| - |F_c||/\Sigma|F_o|$. [b] $wR_2 = \{\Sigma[w(F_o^2 - F_c^2)^2]/\Sigma[w(F_o^2)^2]\}^{1/2}$.

CB2 1EZ, UK; Fax: (internat.) + 44-1223-336-033; E-mail: deposit@ccdc.cam.ac.uk].

[1] C. Oldham, *Carboxylates, Squarates and Related Species*, in: *Comprehensive Coordination Chemistry* (Ed.: G. Wilkinson), Pergamon Press, Oxford, **1987**, chapter 15.6.
[2] A. Caneschi, D. Gatteschi, J. P. Renard, P. Rey, R. Sessoli, *J. Am. Chem. Soc.* **1989**, *111*, 785.
[3] A. K. Majumdar, J. G. SenGupta, *Z. Anal. Chem.* **1958**, *161*, 104.
[4] A. K. Majumdar, J. G. SenGupta, *Z. Anal. Chem.* **1958**, *161*, 181.
[5] G. J. Lamprecht, J. H. Beetge, J. G. Leipoldt, D. R. De Waal, *Inorg. Chim. Acta* **1986**, *113*, 157.
[6] M. Cano, J. V. Heras, M. A. Lobo, M. Martinez, E. Pinilla, E. Gutierrez, M. A. Monge, *Polyhedron* **1991**, *10*, 187.
[7] D. E. Graham, G. J. Lamprecht, I. M. Potegieter, A. Roodt, J. G. Leipoldt, *Trans. Met. Chem.* **1991**, *16*, 193.
[8] G. J. Lamprecht, J. G. Leipoldt, A. Roodt, *Acta Crystallogr., Sect. C* **1991**, *47*, 2209.
[9] M. Cano, J. V. Heras, M. A. Lobo, E. Pinilla, M. A. Monge, *Polyhedron* **1994**, *13*, 1563.
[10] H. M. Haendler, *Acta Crystallogr., Sect. C* **1996**, *52*, 801.
[11] M. A. S. Goher, F. A. Mautner, *Polyhedron* **1993**, *12*, 1863.
[12] H. M. Haendler, *Acta Crystallogr., Sect. C* **1986**, *42*, 147.
[13] W. Li, M. M. Olmstead, D. Miggins, R. H. Fish, *Inorg. Chem.* **1996**, *35*, 51.
[14] U. Brand, H. Varhenkamp, *Inorg. Chem.* **1995**, *34*, 3285.
[15] E. J. Gabe, F. L. Lee, L. E. Khoo, F. E. Smith, *Inorg. Chim. Acta* **1985**, *105*, 103.
[16] M. A. S. Goher, A. K. Hafez, R.-J. Wang, X. Chen, T. C. W. Mak, *Aust. J. Chem.* **1994**, *47*, 1423.
[17] P. Starynowicz, *Acta Crystallogr., Sect. C* **1990**, *46*, 2068.
[18] L. Thommasi, L. Schechter-Barloy, D. Varech, J. P. Battioni, B. Donnadieu, M. Verlest, A. Bousseksou, J-P. Tuchagues, *Inorg. Chem.* **1995**, *34*, 1514.
[19] P. Lainé, A. Gourdon, J-P. Launay, J.-P. Tuchagues, *Inorg. Chem.* **1995**, *34*, 5150.
[20] P. Lainé, A. Gourdon, J-P. Launay, *Inorg. Chem.* **1995**, *34*, 5129.
[21] P. Lainé, A. Gourdon, J-P. Launay, *Inorg. Chem.* **1995**, *34*, 5138.
[22] S. Kiani, A. Tapper, R. J. Staples, P. Stavropoulos, *J. Am. Chem. Soc.* **2000**, *122*, 7503.
[23] R. -G. Xiong, S. R. Wilson, W. Win, *J. Chem. Soc., Dalton Trans.* **1998**, 4089.
[24] Y. Zang, J. Kim, Y. Dong, E. C. Wilkinson, E. P. Appelman, L. Que Jr., *J. Am. Chem. Soc.* **1997**, *119*, 4197.
[25] K. L. Taft, A. Caneschi, L. E. Pence, Ch. D. Delfs, G. C. Papaefthymiou, S. J. Lippard, *J. Am. Chem. Soc.* **1993**, *115*, 11753.
[26] D. Michalska-Fong, P. J. McCarthy, K. Nakamoto, *Spectrochim. Acta* **1983**, *39A*, 835.
[27] K. Nakamoto, *Infrared and Raman Spectra of Inorganic and Coordination Compounds*, John Wiley & Sons, New York, **1997**.
[28] L. J. Bellamy, *The Infrared Spectra of Complex Molecules*, Chapman and Hall, London, **1975**.
[29] G. B. Deacon, R. J. Phillips, *Coord. Chem. Rev.* **1980**, *33*, 227.
[30] R. Boèa, P. Baran, L. Dlhán, H. Fuess, W. Haase, W. Linert, B. Papánková, R. Werner, *Inorg. Chim. Acta* **1998**, *278*, 190.
[31] H. A Goodwin, *Coord. Chem. Rev.* **1976**, *18*, 293.
[32] A. B. P. Lever, *Inorganic Electronic Spectroscopy*, Elsevier, Amsterdam, **1984**.
[33] O. Kahn, *Molecular Magnetism*, VCH Publishers, New York, **1993**.
[34] W. M. Reiff, H. Wong, R. B. Frankel, S. Foner, *Inorg. Chem.* **1977**, *16*, 1036.
[35] H. T. Witteveen, J. Reedijk, *J. Solid State Chem.* **1974**, *10*, 151.
[36] S. J. Gruber, C. M. Harris, E. Sinn, *J. Chem. Phys.* **1968**, *49*, 2182.
[37] A. Abragam, B. Bleaney, *Electron Paramagnetic Resonance of Transition Ions*, Clarendon Press, Oxford, **1970**.
[38] J. C. Gill, P. A. Ivey, *J. Phys. C: Solid State Phys.* **1974**, *7*, 1536.
[39] Cz. Rudowicz, *Phys. Rev.* **1980**, *B21*, 4967.
[40] G. T. Long, D. A. Cleary, *J. Phys.: Condens. Matter* **1990**, *2*, 4747.
[41] D. A. Cleary, A. H. Francis, E. Lifshitz, *Chem. Phys.* **1986**, *106*, 123.
[42] A. Weiss, H. Witte, *Magnetochemie*, Verlag Chemie, Weinheim, **1973**.
[43] *Kuma Diffraction. KM-4 User's Guide*, Version 10.1. Kuma Diffraction, Wrocław, **1998**.
[44] G. M. Sheldrick, *Acta Crystallogr., Sect. A* **1990**, *46*, 467.
[45] G. M. Sheldrick, *SHELXL-97: Program for the Refinement of Crystal Structures*, University of Göttingen, Germany, **1997**.
[46] G. M. Sheldrick, *SHELXA: Program for Post-absorption corrections*, University of Göttingen, Germany, **1997**.

Received May 30, 2003
Early View Article
Published Online October 23, 2003

